Neutron and X-Ray Structure Determination of Laurionite-Type Pb{O(H,D)}X, with X = Cl, Br, and I, Hydrogen Bonds to Lead(II) Ions as a Hydrogen-Bond Acceptor

Heinz Dieter Lutz,[1] Konrad Beckenkamp, Thomas Kellersohn, Hendrik Möller, and Stefan Peter

Universität-GH-Siegen, Anorganische Chemie I, D-57068 Siegen, Germany

DEDICATED TO PROFESSOR HANSKARL MÜLLER-BUSCHBAUM ON THE OCCASION OF HIS 65TH BIRTHDAY

The crystal structures of Pb(OH)Br, Pb(OH)Cl, Pb(OD)Br, and Pb(OD)I have been refined by single-crystal X-ray and neutron diffraction, and neutron powder Rietveld methods, respectively. The laurionite-type structures (*Pnma*, $Z = 4$; $wR_2 = 4.85\%$, $a = 711.2(1)$, $b = 401.92(5)$, and $c = 971.4(1)$ pm (Pb(OH)Cl); $R_w = 9\%$, $a = 738.5(1)$, $b = 408.53(6)$, and $c = 1001.2(1)$ pm (Pb(OH)Br); $R_I = 3.6\%$, $a = 738.38(2)$, $b = 408.433(9)$ and $c = 1001.38(3)$ pm (Pb(OD)Br); $R_I = 6.2\%$, $a = 780.61(2)$, $b = 420.40(1)$, and $c = 1045.88(3)$ pm (Pb(OD)I)) have been confirmed. In contrast to the corresponding barium and strontium compounds, the hydrogen bonds formed are considerably stronger. This is caused by (i) the stronger synergetic effect of lead(II) ions compared to barium and strontium ions and (ii) by the action of the lone pair of Pb^{2+} as a hydrogen-bond acceptor. The existence of a $O(H,D)\cdots Pb$ hydrogen bond is confirmed by cohesive energy calculations with respect to the orientation of the hydroxide ions in the structure. Thus, the OH^- ions are inclined toward the lead ions as compared to the electrostatic potential minimum. © 1996 Academic Press, Inc.

INTRODUCTION

Recently, we studied laurionite-type hydroxy halides $M\{O(H,D)\}X$ with $M = Ba$ and Pb and $X = Cl$, Br, and I and $Sr\{O(H,D)\}I$ by X-ray and partly neutron diffraction, as well as by infrared and Raman spectroscopic methods (1–3). In addition to isostructural (isosymmetric) phase transitions and structural H/D isotope effects (1), this isostructural series exhibits very different behavior with respect to the strengths of the hydrogen bonds formed. Thus, only weak and very weak, if at all, hydrogen bonds are formed in the case of the respective barium and strontium

compounds, whereas rather strong hydrogen bonds are present in the lead compounds $Pb\{O(H,D)\}X$ (3). This behavior was ascribed to the much stronger synergetic effect of lead ions compared to alkaline earth metal ions (4).

In addition, hydrogen bonds like $OH\cdots Pb$, i.e., to the lone pair of the Pb^{2+} ion, were assumed to be present in these compounds (5). In order to confirm or to rule out the physical reality of $OH\cdots Pb$ hydrogen bonds we performed X-ray single-crystal (Pb(OH)Br), neutron single-crystal (Pb(OH)Cl), and neutron powder diffraction experiments (Pb(OD)Br and Pb(OD)I) and cohesive energy calculations on these compounds in addition to the very recently reported (3) infrared and Raman spectroscopic studies. The only structure data available of the title compounds were solved by (partly photographic) X-ray methods (6–9).

EXPERIMENTAL

Polycrystalline samples of laurionite-type lead hydroxy halides were prepared by precipitation from hot aqueous solutions of $Pb(CH_3COO)_2$ with NaX ($X = Cl$, Br, I), and deuterated ones by using D_2O solutions. Single crystals of Pb(OH)Cl and Pb(OH)Br were grown by heating the mother liquor with a small amount of the precipitate for some weeks at 350–360 K.

The X-ray single-crystal intensity data of Pb(OH)Br were collected on an Enraf–Nonius CAD4 diffractometer using graphite-monochromatized MoK_a radiation. The data were corrected for Lorentz and polarization effects. Empirical absorption corrections were performed by ψ scans. The structure was refined by using the program SDP (10).

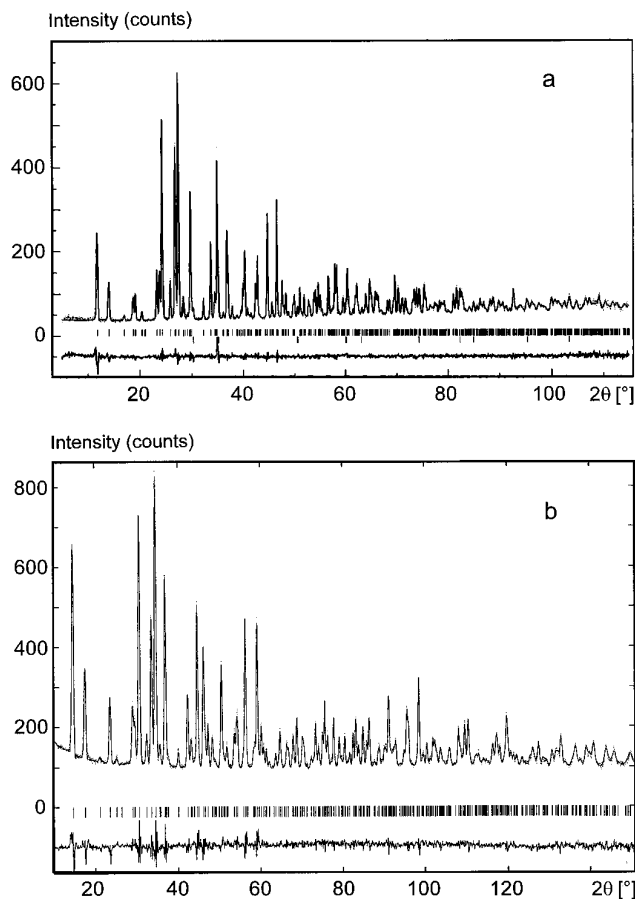[1] To whom correspondence should be addressed.

FIG. 1. Neutron diffraction pattern of Pb(OD)Br (a) and Pb(OD)I (b) at 295 K ($\cdots\cdots$, observed; ——, fitted, difference profile; |, reflections).

TABLE 1

Profile and Structural Parameters of Pb(OD)Br and Pb(OD)I (Neutron Powder Data)

	Pb(OD)Br	Pb(OD)I
Unit-cell dimension (pm)^a		
$a =$	738.38(2)	780.61(2)
$b =$	408.433(9)	420.40(1)
$c =$	1001.38(3)	1045.88(3)
D_{cal} (g cm^{-3})	6.690	6.794
$U(°^2)$	0.242(9)	0.129(6)
$V(°^2)$	−0.249(8)	−0.25(1)
$W(°^2)$	0.108(2)	0.262(4)
Observations	2380	1675
Reflections	503	357
Degrees of freedom	2050	1641
Parameters	25	25
Pseudo-Voigt (Lorentz/Gauß)	0.261	0.128
Asymmetry	0.028/0.036/0.172/−0.001	0.61
$R_{wp}(\%)$	4.3	10.5
$R_I(\%)$	3.6	6.2
$R_{exp}(\%)$	3.3	6.5
χ^2	1.75	2.6
λ (pm)	122.72	159.4
2ϑ (°)	5–115	10–151
Step-width (°)	0.05	0.05

^{a} Obtained from Rietveld refinements.

(ILL), Grenoble (Pb(OD)I), with the samples taken in vanadium containers. The measurements were made with neutron wavelengths λ = 122.72 and 159.4 pm, respectively. After rescaling, refinements of the profile, positional, isotropic, and anisotropic mean square displace-

The neutron single-crystal measurements of Pb(OH)Cl were performed at ambient temperature with the four-circle diffractometer of the Technical University of Darmstadt (research group of Professor Fuess) at the SILOE reactor of the Commissariat à l'Energie Atomique/Centre d'Etudes Nucléaires de Grenoble (CEA/CENG), Grenoble. Because of the small size of the needle-like crystal (0.46 mm^3 in volume) the measuring time was 10 days. The neutron wavelength used was 118.48 pm. After rescaling, refinement of the symmetry-averaged reflections was performed with the program SHELXL-93 (11). As starting parameters the heavy atom positions obtained by the X-ray structure determination (7) were used. The scattering lengths were b(Pb) = 9.4017, b(Cl) = 9.5792, b(O) = 5.805, and b(H) = −3.7409 (12).

The neutron powder diffraction experiments were performed at ambient temperature with the high-resolution powder diffractometers 3T2 at the ORPHEE reactor of the Laboratoire Léon Brillouin (LLB), Saclay (Pb(OD)Br), and D2B at the Institute Laue-Langevin

TABLE 2

Fractional Parameters and Equivalent Thermal Parameters of Pb(OD)Br and Pb(OD)I (Neutron Powder Data; Second Line, X-ray Film Data (9)); All Atoms are on Positions 4c (B_{eq} = 4/3 $\Sigma_i \Sigma_j \boldsymbol{\beta}_{ij}\boldsymbol{\alpha}_i\boldsymbol{\alpha}_j$)

Atom	x	y	z	B_{eq} (10^4 pm^2)
		Pb(OD)Br		
Pb	0.1952(2)	0.25	0.0849(2)	1.58(5)
O	0.3774(3)	0.25	0.4600(3)	1.29(8)
D	0.3002(4)	0.25	0.3845(3)	3.3(1)
Br	0.0522(3)	0.75	0.3191(2)	1.66(7)
		Pb(OD)I		
Pb	0.1824(2)	0.25	0.0812(2)	1.66(8)
	0.178(1)	0.25	0.082(1)	
O	0.3849(4)	0.25	0.4644(3)	1.49(13)
	0.334(14)	0.25	0.436(9)	
D	0.3117(5)	0.25	0.3908(3)	3.71(21)
I	0.0457(4)	0.75	0.3211(2)	1.39(15)
	0.046(3)	0.75	0.320(2)	

TABLE 3

Interatomic Distances (pm) and Angles (°) of Pb(OH)Cl, Pb(OH)Br, Pb(OD)Br, and Pb(OD)I

	Pb(OH)Cl (neutron single-crystal data)	Pb(OH)Br (X-ray single-crystal data)	Pb(OD)Br (neutron powder data)	Pb(OD)I (neutron powder data)
	Pb{O(H,D)}$_3$$X_5${(H,D)O} polyhedra ($X$ = Cl, Br, I)			
Pb^i–$X^{i,ii}$	319.8(2)	328.2(2)	328.4(2)	344.3(3)
Pb^i–X^{iii}	311.2(3)	324.5(3)	325.0(3)	345.0(4)
Pb^i–$X^{iv,v}$	333.8(2)	347.6(2)	347.0(2)	367.6(3)
Pb^i–O^i	379.0(4)	398.7(17)	399.0(4)	430.7(4)
Pb^i–O^{iii,vi}	243.4(2)	245.5(9)	245.4(2)	248.8(2)
Pb^i–O^{vii}	239.2(4)	238.6(16)	238.9(3)	237.0(4)
Pb^i–Pb^{xi,xii}	391.1(4)	391.1(3)	392.1(2)	392.5(3)
X^i–Pb^i–X^{ii}	77.86(6)	76.83(5)	76.90(4)	75.24(6)
$X^{i,ii}$–Pb^i–$X^{iv,v}$	71.27(4)	71.30(4)	71.37(8)	71.77(5)
X^{iii}–Pb^i–$X^{iv,v}$	78.98(7)	77.85(6)	77.93(7)	75.19(6)
X^{iv}–Pb^i–X^v	74.03(9)	71.99(3)	72.10(4)	69.76(5)
$X^{i,ii}$–Pb^i–O^{iii,vi}	77.1(1)	77.2(3)	77.07(11)	77.13(8)
$X^{i,ii}$–Pb^i–O^{vii}	79.06(9)	79.4(3)	79.55(10)	80.9(1)
X^{iii}–Pb^i–O^{iii,vi}	71.8(1)	72.9(3)	73.02(9)	75.07(1)
X^{iii}–Pb^i–O^{vii}	112.7(1)	114.6(4)	114.17(18)	116.4(1)
O^{iii}–Pb^i–O^{vi}	111.3(2)	112.7(5)	112.7(1)	115.4(1)
O^{iii,vi}–Pb^i–O^{vii}	71.8(1)	72.2(2)	71.91(9)	72.20(5)
	Hydroxide ions			
O^i–(H,D)^i	92.1(12)	—	94.7(4)	95.3(5)
(H,D)^i–Pb^i	294.4(7)	—	309.9(4)	339.6(4)
(H,D)^i---$X^{i,ii}$	268.5(6)	—	282.0(3)	304.6(4)
(H,D)^i···$X^{iv,v}$	339.7(6)	—	343.4(3)	356.0(4)
(H,D)^i···X^X	378.7(8)	—	394.7(4)	410.6(5)
O^i---$X^{i,ii}$	329.8(4)	344.7(13)	345.4(3)	369.7(4)
O^i···$X^{iv,v}$	361.2(3)	369.1(14)	369.4(3)	386.0(4)
O^i···X^x	373.4(4)	387.0(17)	386.7(3)	404.2(5)
O^i–(H,D)^i···Pb^i	153.3(6)	—	157.5(13)	160.7(4)
O^i–(H,D)^i···$X^{i,ii}$	124.8(3)	—	125.2(4)	126.9(2)
Pb^{iv}–O^i–(H,D)^i	118.3(5)	—	116.2(4)	115.1(3)
Pb^{vii,ix}–O^i–(H,D)^i	105.4(3)	—	106.0(3)	105.6(2)
Pb^{vii,ix}–O^i–Pb^{iv}	108.2(1)	107.8(4)	108.1(1)	107.75(9)
Pb^{viii}–O^i–Pb^{ix}	111.3(2)	112.7(7)	112.7(1)	115.3(1)

Note. (i) x, y, z; (ii) x, $y - 1$, z, (iii) $\frac{1}{2} - x$, $-\frac{1}{2} + y$, $-\frac{1}{2} + z$; (iv) $\frac{1}{2} + x$, y, $\frac{1}{2} - z$; (v) $\frac{1}{2} + x$, $\frac{1}{2} - y$, $\frac{1}{2} - z$; (vi) $\frac{1}{2} - x$, $\frac{1}{2} + y$, $-\frac{1}{2} + z$; (vii) $-\frac{1}{2} + x$, $\frac{1}{2} - y$, $\frac{1}{2} - z$, (viii) $\frac{1}{2} - x$, $\frac{1}{2} + y$, $\frac{1}{2} + z$; (ix) $\frac{1}{2} - x$, $-y$, $\frac{1}{2} + z$; (x) $-x$, $1 - y$, $1 - z$; (xi) $-x$, $1 - y$, $-z$; (xii) $-x$, $-y$, $-z$.

ment parameters were performed with the Rietveld program FullProf 2.6.1 and PROFIL, respectively (13, 14). The starting values of Pb, Br, I, and O were taken from Refs. (9, 15). The scattering lengths used were b(Pb) = 9.405, b(Br) = 6.800, b(O) = 5.803, and b(D) = 6.671 (16), and b(Pb) = 9.4017, b(I) = 5.28, b(O) = 5.805, and b(D) = 6.674 fm, respectively (12). Some aluminium reflections due to the seal of the sample holder (<2 wt%) were considered in the structure refinement of Pb(OD)Br.

The electrostatic (Madelung) cohesive energies of the laurionite-type hydroxy halides as a function of the orientation of the OH$^-$ ions in the structure were calculated with the program MAPLE (17, 18). The calculations were per-

formed for different effective charges of the atoms involved ranging from +1.35 to +2.0 for M, from −0.8 to −1.0 for X, from −1.0 to −1.46 for O, and from +0.13 to +0.46 for H (19).

RESULTS

The observed and fitted diffraction patterns of Pb(OD)Br and Pb(OD)I are shown in Fig. 1. The final R values based on 2380 and 1675 observations containing 503 and 357 reflections and 2050 and 1641 degrees of freedom are R_{wp} = 4.3 and 10.5%, R_{exp} = 3.3 and 6.5%, R_I = 3.6 and 6.2%, respectively. The final profile

TABLE 4

Crystal Data, Parameters of Data Collection, and Details of Structure Refinements of Pb(OH)Cl and Pb(OH)Br (Neutron an X-ray Single-Crystal Data)

	Pb(OH)Cl Neutron	Pb(OH)Br X-ray
Unit-cell dimension (pm)[a]		
$a =$	711.2(1)	738.5(1)
$b =$	401.92(5)	408.53(6)
$c =$	971.4(1)	1001.2(1)
D_{cal} (g cm^{-3})	6.21	6.69
Crystal dimensions (mm)	$3.2 \times 0.48 \times 0.30$	$0.18 \times 0.16 \times 0.14$
Wavelength used (pm)	118.48	71.069
$F(000)$	88	504
μ (cm^{-1})	<0.01 (cal.)	691.55
2ϑ (°)	6–96	1–80
$(\sin \vartheta/\lambda)_{max}$ (pm^{-1})	$6.272 \cdot 10^{-3}$	$9.033 \cdot 10^{-3}$
h_{min}, h_{max}	−4, 1	0, 13
k_{min}, k_{max}	−8, 8	0, 7
l_{min}, l_{max}	−11, 11	0, 18
Standard reflections	0 3 1	4 3 0, 2 0 9, 0 3 7
No. of reflections measured	1179	1130
No. of unique reflections	221	1030
Cut-off	—	I = 4.5 σ_I
No. of refined reflections	221	838
Parameters refined	26	20
Refinement on	F^2	F
Agreement factors R (%)		
($I > 2\sigma_I$)	R_1:3.16, wR_2:4.85	8.1[b]
(all data)	R_1:6.33, wR_2:5.45	9.0[c]
Weighting scheme	$1/[\sigma^2(F_0^2 + (0.0223\ P)^2]^d$	unit weights
Goodness-of-fit	1.014	2.22
Extinction coefficients	0.063(6)	$1.22(4) \times 10^{-6}$

[a] Obtained from X-ray Guinier photographs.
[b] R.
[c] Rw.
[d] $P = (F_0^2 + 2F_c^2)/3$.

parameters are given in Table 1, and the structural parameters in Table 2. Selected distances and angles are given in Table 3.

The crystal data and the data of structure refinement of Pb(OH)Cl (neutron) and Pb(OH)Br (X-ray) single crystals are given in Table 4, the fractional atomic coordinates in Table 5,[2] and the anisotropic thermal parameters in Table 6. Selected distances and angles are given in Table 3.

The laurionite-type structures of the title compound reported in the literature (6–9) have been confirmed.

The coordination geometries of the Pb^{2+} ions and those of the OH$^-$ and OD$^-$ ions are shown in Figs. 2 and 3.

The results of the cohesive energy calculations are shown in Figs. 4 and 5 and Table 7. They reveal that the OH$^-$ ions are inclined toward the lead ions as compared to the electrostatic potential minimum whereas in the corresponding alkaline earth compounds the hydroxide ions are repelled from the metal ions.

DISCUSSION

As shown in Fig. 3, in the case of laurionite-type lead compounds the hydrogen or deuterium atoms of the OH(D)$^-$ ions are orientated in direction of adjacent Pb^{2+} ions in contrast to the isostructural barium (and strontium) compounds. In the latter case, the hydroxide

TABLE 5

Fractional Atomic Coordinates and Isotropic Thermal Parameters of Pb(OH)Cl and Pb(OH)Br (Neutron and X-ray Single-Crystal Data; Second Line, X-ray Literature Data (7, 8); All Atoms are on Positions $4c$; $B_{eq} = 4/3\ \Sigma_i\ \Sigma_j\ \beta_{ij}\ \alpha_i\ \alpha_j$)

Atom	x	y	z	$B_{eq}(10^4\ pm^2)$
		Pb(OH)Cl (neutron data)		
Pb	0.2030(3)	0.25	0.0879(2)	1.68(8)
	0.20264(9)	0.25	0.08770(7)	1.32(2)
O	0.3725(5)	0.25	0.4578(4)	1.45(16)
	0.378(2)	0.25	0.458(1)	1.2(4)
H	0.291(1)	0.25	0.3840(7)	4.4(3)
Cl	0.0563(3)	0.75	0.3204(2)	1.74(8)
	0.0564(6)	0.75	0.3202(4)	1.16(1)
		Pb(OH)Br (X-ray data)		
Pb	0.1947(1)	0.25	0.0844(1)	0.95(1)
	0.197	0.25	0.084	
O	0.377(2)	0.25	0.459(2)	0.7(2)
	0.394	0.25	0.456	
Br	0.0524(3)	0.75	0.3193(3)	1.00(3)
	0.048	0.75	0.320	

FIG. 2. Coordination geometries of the lead ions in laurionite-type Pb(OD)Br (probabilities 50%).

ions are orientated to adjacent halide ions forming very weak (if at all) OH$\cdots\cdot X$ hydrogen bonds (X = Cl, Br, I) (1, 2). Therefore the question arose if there are OH$\cdots$Pb hydrogen bonds via the lone pair of the lead ions (5).

The hydrogen bonds formed in the laurionite-type lead compounds are much stronger as revealed by infrared and Raman spectroscopic experiments. Thus, the respective OH and OD stretching modes range from 3498 to 3518 and from 2584 to 2598 cm^{-1} (all 295 K) instead of >3590 and >2648 cm^{-1} found for the alkaline earth metal halides (3). The stronger hydrogen bonds of the lead compounds compared to the those of the former were ascribed to the

stronger synergetic effect of Pb^{2+} ions compared to Ba^{2+} and Sr^{2+} ions (4).

On the other hand, the hydrogen bonds present in the hydroxy lead halides are stronger than inferred from the respective H(D)$\cdots X$ distances as revealed from the $\nu_{OH(D)}$ vs H(D)$\cdots X$ correlations curves reported in the literature (20). According to these correlations, hydrogen bonds due to H(D)$\cdots X$ distances of 268.5, 282.0, and 304.6 pm for X = Cl, Br, and I, respectively, must be much weaker than those revealed by the OH(D) stretching modes irrespective of the increase in strength of hydrogen bonds in the case of bifurcated bonds (2–4, 21). The latter would correspond to distances in the range of about 250, (265), and 275 pm. We therefore assume the hydrogen bonds present are at least partly caused and reinforced by interactions with the lone pair of the lead ions.

This is confirmed by the cohesive energy calculations. Thus, the orientations of the hydroxide ions in Pb(OH)X deviate from those calculated by 2.5°–5.0° (depending on the compound under study, the ionic charges chosen, and the calculation procedure used). In the case of the corresponding laurionite-type alkaline earth compounds, the respective angles also deviate but by up to 3.2° in the opposite direction (see Figs. 4 and 5 and Table 7). Hence, in all laurionite-type lead compounds, the OH$^-$ ions are inclined from the electrostatic potential minima toward

TABLE 6

Anisotropic Thermal Parameters ($U_{ij}/100\ pm^2$) of Pb(OH)Cl and Pb(OH)Br

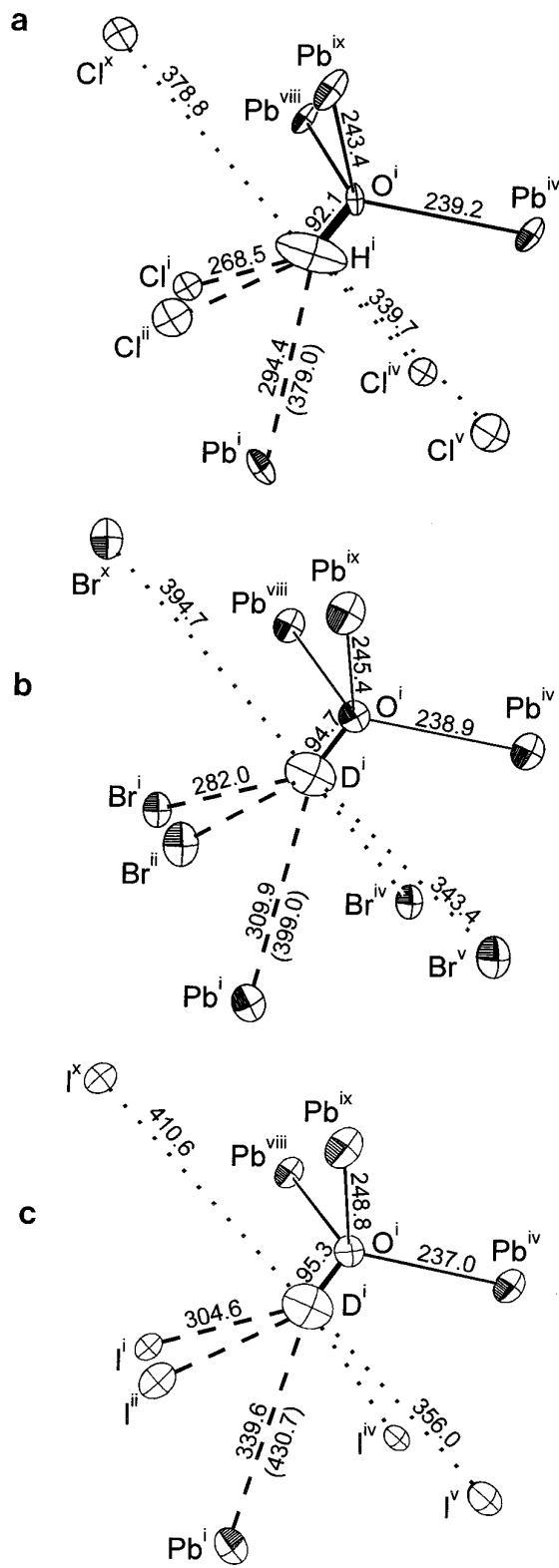| Atom	U_{11}	U_{22}	U_{33}	U_{13}
	Pb(OH)Cl (single-crystal neutron data)			
Pb	1.9(1)	1.8(1)	2.7(1)	−0.9(1)
Cl	1.7(1)	2.5(1)	2.4(1)	0.1(1)
O	1.5(2)	2.0(2)	2.0(2)	0.1(2)
H	5.4(4)	8.2(5)	3.0(4)	−1.1(4)
	Pb(OH)Br (single-crystal X-ray data)			
Pb	1.20(2)	0.77(2)	1.65(3)	−0.77(3)
Br	1.14(8)	1.21(8)	1.46(9)	0.01(8)
O	0.7(5)	1.0(6)	1.1(6)	0.1(5)

FIG. 3. Coordination geometries of the OH⁻ and OD⁻ ions in Pb(OH)Cl (a), Pb(OD)Br (b), and Pb(OD)I (c) (neutron single-crystal and neutron powder data; distances, pm; probabilities 50%).
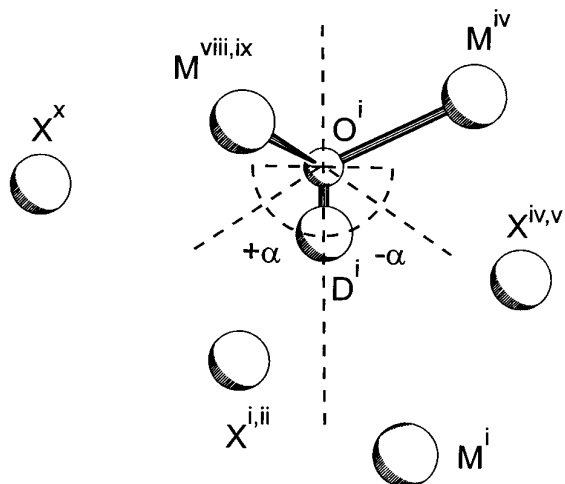

FIG. 4. Orientation of the hydroxide ions in laurionite-type hydroxide halides; the angle α describes deviations from the experimentally observed orientation within the mirror plane of the structure.
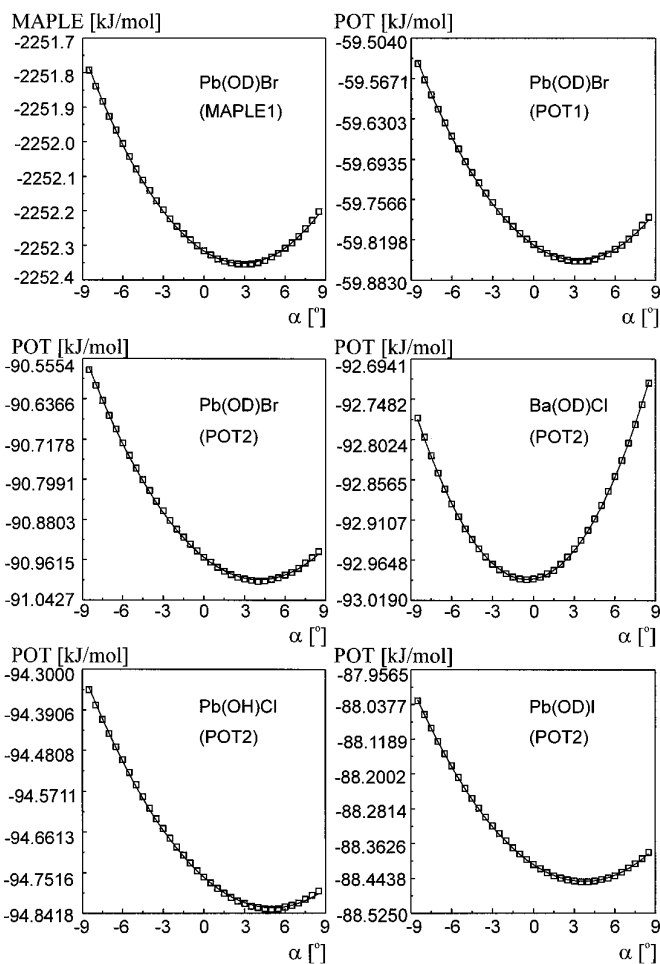

FIG. 5. Madelung parts of the cohesive energies of the crystal (MAPLE, kJ mol⁻¹) and electrostatic potentials at the site of the proton (POT, kJ mol⁻¹) versus the angle α as defined in Fig. 4 (see Table 7).

TABLE 7

Angles $\Delta\alpha$, i.e., Deviation of the Orientation of the Hydroxide Ion from the Experimental One (see Fig. 4), of Laurionite-Type Hydroxide Halides Calculated for Various Ionic Charges of the Atoms Involved; $\Delta\alpha$ Obtained for the Minimum of the Electrostatic Part of the Cohesive Energy (MAPLE) and for Minimum of the Madelung Potential at the Position of the Hydrogen Atom (POT), Respectively

	Pb(OD)X			Ba(OD)X				
X	Cl[a]	Br	I	Cl	Cl[b]	Br	I	Sr(OD)I
POT 1	4.2	3.2	2.7	0.0	−1.0	−1.3	−2.7	−1.3
MAPLE 1	4.0	2.8	2.5	0.2	−1.1	−1.2	−3.2	−1.5
POT 2	5.0	4.0	3.7	−0.5	−0.8	−1.1	−2.5	−1.5
MAPLE 2	4.1	2.8	2.5	0.0	−0.8	−1.6	−3.2	−2.2

Note. The ionic charges chosen are for 1: $M^{+1.80}$, $X^{-0.8}$, $O^{-1.13}$, $H^{+0.13}$ and for 2: $M^{+2.00}$, $X^{-1.0}$, $O^{-1.45}$, $H^{+0.45}$. Calculations for $M^{+1.35}$, $X^{-0.8}$, $O^{-1.00}$, $H^{+0.45}$, $M^{+1.80}$, $X^{-0.8}$, $O^{-1.46}$, $H^{+0.46}$, and $M^{+1.65}$, $X^{-0.8}$, $O^{-1.00}$, $H^{+0.15}$ see (19).
[a] Pb(OH)Cl.
[b] Data for 1.5 K.

the adjacent Pb^{2+} ions whereas in the case of the barium and strontium compounds, the protons are repelled from the metal ions.

If O⁻H···Pb hydrogen bonds are formed the question arises why the strengths of the bonds increase on going from the laurionite-type lead chloride to the iodide as shown from the respective OH stretches (see above) whereas the corresponding (H,D)···Pb distances increase in the same direction from 294.4 to 339.6 pm. There are two explanations possible. (i) The strengths of bifurcated hydrogen bonds to adjacent halide ions, which must be considered additionally (3), increase on going from the chloride to the iodide. (ii) The size of the Pb^{2+} lone pairs increase in the same direction revealing increasing directionality of the lone pair. The latter explanation is reasonable because in the case of the iodide the respective lead halide distances are larger (344–368 pm) than those of the bromide (325–347 pm) and the chloride (311–334 pm). The Pb–O distances due to the (H,D)···Pb hydrogen bonds are 379.0, 398.7, and 430.7 pm smaller than that of red PbO via the lone pair (432.5 pm (22)).

REFERENCES

1. H. Möller, K. Beckenkamp, Th. Kellersohn, H. D. Lutz, and J. K. Cockcroft, *Z. Kristallogr.* **209,** 157 (1994).
2. St. Peter, J. K. Cockcroft, T. Roisnel, and H. D. Lutz, *Acta Crystallogr. B,* in press.
3. H. D. Lutz, K. Beckenkamp, and St. Peter, *Spectrochim. Acta A* **51,** 755 (1995).
4. H. D. Lutz, *Struct. Bonding (Berlin)* **69,** 97 (1988).; *Struct. Bonding (Berlin)* **82,** 85 (1995).
5. H. Möller, K. Beckenkamp, Th. Kellersohn, and H. D. Lutz, *Z. Kristallogr. Suppl.* **5,** 165 (1992).
6. H. Brasseur, *Bull. Soc. R. Sci. Liège* **11,** 166 (1940).
7. C. Ch. Venetopoulos and P. J. Rentzeperis, *Z. Kristallogr.* **141,** 246 (1975).
8. Ch. Knakkergård Møller, *Mat. Fys. Medd. Dan. Vid. Selsk.* **35,** 14 (1966).
9. R. Näsänen, *Suomen Kemistilehti B* **39,** 105 (1966).
10. Enraf-Nonius, Structure Determination Package (SDP), Frenz & Associates, Inc. College Station, Texas, and Enraf-Nonius, Delft (1988).
11. G. M. Sheldrick, SHELXL-93, Program for Crystal Structure Refinement, Univ. Göttingen (1993).
12. L. Koester and H. Rauch, Summary of neutron scattering lengths, IAEA-Contact 2517/RB (1983).
13. J. Rodriguez-Carvajal, "Abstract of the Satellite Meeting on Powder Diffraction of the XV Congress of the IUCr, Toulouse, France," p. 127. 1990.
14. J. K. Cockcroft, "PROFIL, A New Rietveld Program with Chemical and Thermal Restraints." Institute Laue-Langevin, France, Program Library, Version 4.05 (1991).
15. Th. Kellersohn, Ph.D. Thesis, University of Siegen (1990).
16. V. F. Sears, *in* "Neutron Scattering (K. Sköld and D. L. Price, Eds.), *Methods of Experimental Physics* **23A,** 521 (1986).
17. R. F. Giese, *Z. Kristallogr.* **146,** 205 (1977).
18. R. Hübenthal and R. Hoppe, "MAPLE, Madelung Part of Lattice Energy." University of Gießen (1989).
19. H. Möller, Ph.D. Thesis, University of Siegen (1993).
20. W. Mikenda, *J. Mol. Struct.* **147,** 1 (1986).
21. H. Möller, Th. Kellersohn, M. Schmidt, H. D. Lutz, and J. K. Cockcroft, *Z. Kristallogr.* **208,** 19 (1993).
22. P. Boher, P. Garnier, J. R. Gavarri, and A. W. Hewat, *J. Solid State Chem.* **57,** 343 (1985).